HUMAN FEMUR RESPONSE TO IMPACT LOADING

Kress, Tyler A.[1], John N. Snider[1], David J. Porta[2],
Peter M. Fuller[2], Jack F. Wasserman[1], Guy V. Tucker[1]

Abstract

This paper presents some of the results of a research project entitled "Dynamic Response of the Human Leg to Impact Loading." A test facility was developed for laboratory experimentation that simulates leg impacts during automobile, pedestrian, motorcycle, and bicycle accidents. Analyses and discussions are presented for several experiments designed to study the mechanical behavior of the human femur subjected to impact loading.

About one-hundred bones have been broken in the specially designed laboratory as part of this research. The testing was divided into four categories: (1) femurs subjected to bending loads, (2) femurs under torsional loads, (3) femurs under axial loads, and (4) fresh tissue impact loadings.

The femur appears stronger when impacted in the anterior-to-posterior (a-p) direction than when impacted in the lateral-to-medial (l-m) direction. The fractures produced by the a-p impacts provide interesting clinical information. It was found that even very small torsional preloads can greatly diminish the femurs breaking strength. Axially loading the femur allowed mapping of the stress along the femur to accurately predict fracture locations.

Femur and intact thigh tests are continuing and these results will be supplemented in the future. This paper presents the implications of the first designed series of tests.

Introduction

The work reported on in this paper is part of a research project entitled "Dynamic Response of the Human Leg to Impact Loading," being jointly conducted by the University of Tennessee and the University of Louisville. The intent of the research project is to describe and quantify the dynamic response of the human leg to impact loadings as encountered when pedestrians or cyclists are struck by automobiles. The approach has been to develop a test facility that simulates collisions between automobiles and pedestrians, motorcycles, or bicycles. The facility was designed so that it would produce leg injuries comparable to those normally seen in a clinical setting.

Progress made since the introduction of the research in 1986 has been significant and includes the design and installation of a state-of-the-art impact testing laboratory; the completion of impact tests using human legs, animal legs, and simulated leg structures; and development of a basic understanding of the response of the human leg to impact loading. Other contributions include appropriate biological and structural material testing, development efforts for a computer-based simulation of lower leg response to impact loading, clinical studies of accidents involving traumatic leg injury, statistical studies of traumatic injuries, whole body vibration research, underwater impact injury studies, head impact tolerance and experimental injury research, various accident reconstruction projects, causal mechanism analyses of human injury, and other biomechanical laboratory experimentation.

This paper presents some results for the purposes of understanding fracture behavior of the human femur during impact loading.

Methodology

The biomechanics test facility discussed in the introduction was used for the experiments. The impact machine used for most of the tests will be referred to in this paper as the crash simulator. The three principle parts of the crash simulator are the accelerator and cart, the specimen holding device, and the force measurement system.

The simulator is a pneumatically-powered machine used to simulate a car/motorcycle or car/pedestrian collision. A cart of significant mass (50 kilograms) is propelled down a rail system where it impacts a test specimen (e.g. a human bone, a human leg, an animal bone or an artificial bone). The cart is instrumented with a force measurement system enabling the user to obtain dynamic force information during impact.

[1] Engineering Institute for Trauma and Injury Prevention
153 Alumni Memorial Building
University of Tennessee
Knoxville, Tennessee 37996-1506 USA

[2] Department of Anatomical Sciences & Neurobiology
HSC-A Room 915
University of Louisville School of Medicine
Louisville, Kentucky 40292 USA

A 4.1275-centimeter (1 5/8-inch) pipe or a 7.62 x 20.32 x 0.3175 centimeter (3 x 8 x 1/8 inch) plate mounted on the cart serves as the impacting surface. Data from each test using the crash simulator is obtained via a force transducer mounted on the impact cart. The transducer is mounted in such a way that during impact it "feels" the same reaction that the test specimen does. The pipe or plate is held on by slide pins which allow all of the force to be transferred to the force transducer. The force transducer is manufactured by PCB Piezoelectronics, model number 208A04. The sensitivity of the transducer is 1.16 kilonewtons per volt.

The signal from the force transducer passes through a PCB Power Unit and then to a Hewlett-Packard 3562a Dynamic Signal Analyzer where the force versus time history of the event is recorded.

For this study, four different types of tests using the crash simulator were conducted on the femur. These tests involved utilizing four separate support/specimen holding structures: simply-supported (pinned-pinned) bone loaded in the anterior-posterior direction; simply-supported bone loaded in the lateral-medial direction; simply-supported bone with a torsional preload; and axially loaded bone.

Ninety-four bones were obtained for use in this study. Eighty of the bones were embalmed[3] femurs with soft tissue removed. The other fourteen bones were fresh, cryogenically frozen long bones from two recently deceased persons. Demographic information was available for some of the bones. The fresh frozen bones were thawed in a saline water bath just prior to testing.

A key objective of this study was to understand the mechanical behavior of the femur during impact, therefore a number of different loading conditions were applied to the bones. These different conditions can be described by dividing them into four types of tests: 1) bending, 2) torsional, 3) axial, and 4) fresh tissue tests.

In all tests except the low strain rate axial tests and the steady state torsional tests, the crash simulator was used. Data was recorded in the form of a force-time plot, an example of which is shown in **Figure 1**.

The breaking force, the amount of time from impact initiation to fracture, and the area under the curve were obtained from each force-time curve. The breaking force was used to calculate, among other things, the ultimate stress. The time measurement allows for the calculation of displacement since there is a constant velocity through impact. The area under the curve is directly related (by the reciprocal of the volume) to the amount of energy absorbed during impact and is used strictly for comparison with other tests.

Prior to testing, certain anatomical measurements were made on the bones. Following testing, cortical thickness measurements were taken.

Protocol, justification and procedure for each test is detailed below.

Test Series I: Breaking Strength of Femur

An automobile impact onto the side of a motorcycle is primarily a lateral-medial type of impact.

Lateral-medial loadings of bare femurs were accomplished using the crash simulator at a speed of approximately seven meters per second. A "simple support, l-m loading" holding device was developed and used for these tests. Twelve femurs were tested.

The breaking force was determined for each bone from the force-time plot. The breaking forces for the twelve bones were averaged to determine a bone tolerance level. Kress (1989) reported good correlation between breaking strength and cortical thickness of long bone impact tests. First and second order curves were fit to the femur data.

Using the breaking force and the anatomical measurements taken for each bone, the ultimate bending stress can be approximated using beam theory.

The formula for calculating bending stress is

$$\sigma_{b(max)} = M_{(max)}\, c / I$$

where σ_b = bending stress, M = bending moment, c = distance from centroid to edge of beam, and I = moment of inertia.

For a simply-supported beam loaded in the center, the maximum moment is

$$M_{(max)} = PL/4$$

where P = breaking force and L = distance between supports.

For the femur calculations, the shaft will be considered a perfect cylinder with an outer radius, r_o, and an inner radius, r_i, with

[3] The embalming fluid consisted of the following: 20% Isopropyl Alcohol (99%); 20% Propylene Glycol USP; 4% Formaldehyde; 37% (Formalin); 4% Phenol; 52% Tap Water; majority of cadavers embalmed within eighteen hours of death (maintained in cooler until embalmed).

$$r_i = r_o - t$$

where t is the cortical thickness. The cortical thickness is measured at six points at midshaft and averaged. Other researchers have supported this method (Viano and Khalil, 1976; and Moore, 1985). This distance from a centroid to edge of bone, c, is simply r_o, and I is given by

$$I = [\pi/4]\,(r_o^4 - (r_o - t)^4)\,.$$

In addition to bending stress, Young's modulus can be approximated using beam theory. The equation for maximum deflection of this beam

$$\delta_{max} = PL^3/48EI$$

can be written as

$$E = PL^3/48\delta I$$

where E = Young's modulus and δ = maximum defection.
The maximum deflection is found by multiplying time of contact until fracture occurs by striker velocity, since there is no significant change in the striker velocity through the event. This calculation only gives an approximation for Young's modulus because the equation used is only valid for uniform cross-sectional bodies.

The area under the force-time curve is calculated to represent the relative energy absorption. The types of fractures that occurred were recorded.

Anterior-posterior loading of the femur is a common occurence. It is most often associated with airborne bodies. Testing the femur in this direction was also of academic interest, because bone is non-homogeneous, anisotropic, and has complex, varying geometry.

Much of the procedure for this type of test was the same as for lateral-medially loaded femurs except that a "simple-support, a-p loading" holding device was used and 32 femurs were tested.

Demographic information was available for these bones, making it possible to study age effects on the fracture behavior of the bone. In addition, this testing allowed for a comparison to be made between the behavior of left and right femurs of the same person.

Test Series II: Torsional Strength of Femur

Six femurs were available for determination of the maximum, slowly-applied torque to produce failure. Gradually increasing torsional forces were applied until the bones fractured.

The maximum torsional stress is calculated as (remember the femur shaft is being considered as a hollow circular cylinder)

$$\tau_{(max)} = T_{(max)}\,c/J$$

where τ = shear stress, T = torque, c = distance from centroid to outer edge of bone (r_o), and J = polar moment of inertia,

$$J = [\pi/2]\,(r_o^4 - (r_o - t)^4)\,.$$

It is suspected that the legs of motorcycle riders undergo multiple loading configurations when suffering a collision.

To begin to understand the effects of these multiple loads, combined torsion and bending tests were performed. A torsional preload was placed on a simply-supported femur. The femur was then impacted at high-speed in the lateral-medial direction with the crash simulator.

To best understand the effect of the torsional preload, matched pairs of femurs were used. The right femur was struck in the l-m direction with no torsional preload. The left femur was struck similarly but with a torsional preload.

Test Series III: Compressive Strength of Femur

Although several researchers have investigated the compressive strength of the entire thigh, few, if any, have loaded a whole, bare femur in the axial direction at low (steady-state) and high speeds (7.6 meters per second). Eighteen bones were tested under such conditions.

A materials testing machine was employed to test nine bare, embalmed femurs in axial compression to failure. Cups simulating the acetabulum and the tibial plateau were designed to fit the machine and allow a distributed load on the condyles and head of the femur. The only data measured was the breaking forces. Video and photographic documentation allowed for the analysis of fractures.

Using the breaking force and the anatomical measurements, breaking strength can again be approximated using beam theory. Due to the geometry of the femur, an axial load is not truly an axial load. A bending element is also involved. The stress when bending and axial loads are involved is given by

$$\sigma_x = (\sigma_x)_{centric} + (\sigma_x)_{bending} = P/A \pm Mc/I$$

where P = force, A = cross-sectional area, M = bending moment, c = distance from centroid, and I = moment of inertia.

If axially loaded, the centric effect on the femur is completely compressive. However, the bending effect will impose compression on the medial side and tension laterally. Therefore the stress in the bone is given by

$$\sigma_x = P/A + Mc/I \quad (medial) \quad and \quad \sigma_x = P/A - Mc/I \quad (lateral).$$

It should be noted that these calculations are approximations. Mc/I does not hold when E, tension, does not equal E, compression. The E's are close enough in the bone (four percent according to Evans, 1951), however, that this does not significantly change the results. Also, it should be noted that the neutral axis is not the same as the centroidal axis.

Stresses were calculated at three cross-sections on the bone: at midshaft, just below the greater trochanter, and at the neck of the femur (see **Figure 2**). The cross-section of minimum moment of inertia was chosen at each area.

The breaking force, P, and cross-sectional areas are taken directly from measurements. The bending moment, M, is equal to Pd (M = Pd) where d = moment arm. A hollow cylinder cross-section is assumed as before.

In order to examine high speed loading of the femur in the axial direction, nine femurs have been impacted in the crash simulator. The axial loading, specimen holding device was used. The flat plate impactor was used instead of the pipe.

Measurements and calculations for these tests were the same as for the statically loaded bone.

Test Series IV: Fresh Tissue Testing

The type of preservation technique used on the tested bones affects the properties of the bones. In an effort to begin to examine these effects, 14 fresh bones were tested in the crash simulator. These bones were cryogenically frozen just after death and were wet-thawed shortly before testing.

Breaking force and area-under-curve data were obtained for each bone. Anatomical measurements were not taken due to the disease risks of the bones utilized.

Results and Discussion

Results from 94 bone-breaking tests are presented. Embalmed, bare femurs have been broken at high speeds (approximately seven meters per second) in the lateral-medial, anterior-posterior, and axial directions. Bone fracture tests have also been performed for steady-state force application in the axial direction and in torsion. Other conditions have included impacting in the lateral-medial direction while the bones are subjected to a torsional preload and a series of fresh bone tests.

Test Series I: Breaking Strength of Femur

Twelve femurs have been impacted in the crash simulator in the lateral-medial direction. Their average cortex thickness was 0.00691 meters and average breaking force was 3053 Newtons (N). Anatomical measurements were not available for three of the bones, and force signals were not obtained for three bones. Linear regression was used to develop a relationship between breaking force and average cortex thickness, and

the correlation coefficient was 0.61. The second order correlation coefficient improves to 0.82. The least squares relationship is

$$Breaking\ Force\ (N) = -22 + 52 \times cortex^2\ (mm).$$

The ultimate bending strength and Young's modulus were calculated by the method described in the methodology section. The average breaking force was 3053 Newtons; the average bending strength was 147 Megapascals; and the average Young's modulus was 30 Gigapascals. These values compare favorably to values found in previous literature.

The average area under the force-time curve is 2236 N-ms. This value is difficult to interpret. It is, however, related to the amount of energy absorbed during impact and can be compared to other area under force-time curve calculations.

Six of the twelve fractures were comminutions (see **Table 1**). Most of the comminutions produced tension wedges, that is the fracture started on the tension side of the bending bone. Oblique and spiral fractures occurred. The spiral fractures were probably caused hy the specimen holding device which also served as a torsional delivery system. Its configuration alone may have encouraged a spiral fracture. One bone that had severe osteoporosis shattered upon impact.

Effects of impact direction on the properties of the bone were investigated hy turning the femurs 90 degrees and striking them in the anterior-posterior direction. The crash simulator was used to break 32 femurs in this manner. Anatomical measurements, support distance, and breaking force data for all of the bones tested were recorded. The average cortex thickness was 0.00739 meters and the average breaking force was 5697 Newtons. The linear regression between breaking force and cortex thickness had a linear correlation coefficient of 0.40. The second order correlation was 0.42 only improving the relation slightly. Therefore the linear regression polynomial curve fit equations for these tests will not he provided.

The ultimate bending stress and Young's modulus were calculated. The average bending stress was 284 Megapascals, and the average Young's modulus was 88 Gigapascals.

Ages of specimens ranged from 53 to 89 years old. Ultimate Bending Stress and Young's Modulus were compared and the scatter of data indicated no real age dependence in this range of age.

The breaking stress of right and left matched pairs of femurs (two femurs belonging to the same individual) were compared. The result, surprisingly, is that the left bone is roughly eight percent stronger on average than the right bone. However, a closer examination of the data reveals that two sets of bones had the left one much stronger than the right (for whatever reason). Discarding these two sets from the averaging results in virtually equal strength for right and left bones.

Area under the force-time curve for each bone was determined. The average value is 2658 N-ms. The value for the 1-m loaded femurs was 2254 N-ms. The a-p loaded bone, therefore, does not absorb much more energy than the 1-m loaded bone, although the strength is much greater in the a-p direction.

Seventy-one percent of the fractures in this a-p test were comminuted (see **Table 2**). Interestingly, however, few produced tension (3) or compression (2) wedges. The vast majority (17) of the comminuted fractures were side wedges. The side wedges were equally dispersed as lateral and medial wedges. Eight fractures were oblique, and one was a shatter.

Test Series II: Torsional Strength of Femur

Six femurs were loaded in torsion at low strain rates. The average cortex thickness, support distance and maximum torque for each bone is presented in **Table 3**. The linear relation, with a correlation coefficient of 0.90, between maximum torque and cortex thickness is given by

$$Maximum\ Torque\ (N\text{-}m) = 6 + 15 \times cortex\ (mm).$$

Using a polynomial curve fit improves the relation to 0.92. The least squares fit is

$$Maximum\ Torque\ (N\text{-}m) = 49 + 1.2 \times cortex^2\ (mm).$$

Ultimate torsional stress was calculated. The average hreaking torque of 108 N-m is slightly lower than Yamada's (1971). If, however, bone six is removed from the average, the breaking torque comes up to 125 N-m. Bone six was highly osteoporotic.

The torsional strength of 28 MPa is also lower than Yamada's value of 45 MPa. This is attributed to our use of embalmed (and perhaps older) bones rather than fresh, wet bones used by Yamada.

Five of the six femur fractures were spiral. The osteoporotic bone six shattered.

The question of combined loads on the femur was investigated by loading six bones in torsion and in bending. A torsional preload was placed on the bones, which were then impacted in the lateral-medial direction by the crash simulator.

Cortex thickness, support distance, amount of preload and breaking force are shown in Table 4. Notice that two different torque levels were used.

All six bones used in these tests were the matching pairs to the six bones tested in the lateral-medial direction without a torsional preload. The average breaking force with no torsional preload was 2549 Newtons. The average with a preload was 2179 Newtons.

After data manipulation, it was determined that on the average, a 14 percent torsional preload decreases the breaking force 14 percent. Interestingly, spiral fractures are present in 50 percent of these preloaded bones.

Test Series III: Compressive Strength of Femur

Nine femurs were loaded at low strain rates in the axial direction using a materials testing machine. The output from the machine is a force reading.

From the ultimate load and anatomical measurements, stresses can be calculated. Since fractures under these loading conditions occur most frequently at three locations (midshaft, sub-trochanter, and neck), stress calculations at all three of these cross-sections were made for each bone.

The six calculated stress values for each bone were recorded on figures as illustrated generally in **Figure 2**. There were two calculated values (lateral and medial) for each of the three locations. Stresses on the lateral side of the bone are tensile and are compressive on the medial sides. Based on the stresses, predictions were made for the fracture location. On eight of the nine femurs the prediction is correct. Bone #881R was the only incorrectly predicted fracture. On this test the cup holding the head of the femur was impinging its neck leading to fracture at that site. In all cases the compressive stress is approximately 1.5 times greater than the tensile. 77.8% of the fractures occured on the neck, 11.1% were sub-trochantric, and 11.1% were simultaneous neck and shaft fractures.

High speed axial impacts of the bare femur were of interest next. Nine bones were struck in this matter; six provided good force data.

Stresses were calculated, mapped, and examined on these bones as previously done. In these cases, all predictions for fracture locations were correct. The only minor exception was a concomitant shaft fracture along with the predicted neck fracture in bone #862L. Such concomitant fractures are common clinically (Chapman, 1984). Once again, the compressive stresses are 1.5 times greater than the tensile. 66.7% of the fractures were in the neck, 16.7% were sub-trochantric, and 16.7% were in the shaft.

Test Series IV: Fresh Tissue Testing

Fourteen cryogenically-frozen, fresh long bones were broken to help understand the effects of embalming on the properties of the bone.

Table 5 presents the results of these tests. When compared to the embalmed data, breaking force values appear to increase 44 percent for fresh femurs and 78 percent for fresh tibias. Energy absorption also increases for fresh bones. There is, however, too little data to make definitive conclusions.

Summary of Recorded and Calculated Response Characteristics

Table 6 presents a summary of the test conditions and recorded data for all of the different tests that have been performed to date utilizing the femur.

Table 7 contains some calculated response characteristics from data obtained in selected femur tests.

If a discrepancy is noticed between certain n values, it should be noted that some of the data, due to their specious nature, were excluded from calculations.

Conclusions

This paper has presented data on the impact response of the human femur under several loading conditions. The data presented are important, because of the role they can play in the quantification of the damage to hard and soft tissue under loading conditions similar to those which occur when an automobile impacts a human leg. Tbe data provides insight into protection mechanism design and input for computer and physical models. The results of each test series are discussed below.

Test Series 1: Breaking Strength of Femur

From the data, it is apparent that the femur is stronger and stiffer when impacted in the anterior-posterior direction than when impacted in the lateral-medial direction. Bone is non-homogeneous, anisotropic and has properties that vary according to location on the bone (Evans, 1951). This directional change in properties, therefore, should be expected.

Bone develops in such a way that it is stronger in areas encountering greater stress. Since normal body activities (walking, running, etc.) put a moment on the femur similar to three-point loading in the a-p direction, this strength increase in the a-p direction can be expected.

No notable effects of age vs. strength or of age vs. stiffness were evident. While it is acknowledged that 20-year-old bones on the average would be stronger than 80-year-old bones, no such statement can be made for the age span of the specimens in this study (53 to 89 years old).

Mather (1968) showed that the left and right femurs absorbed the same amounts of energy when impacted. It was further shown in this report that left and right matched pairs have essentially equal properties (with only a few exceptions). This finding adds validity to many past experiments involving testing of matched pairs of bones. Comments about the resultant fractures from bending impact tests may be of interest. The lateral-medial impacts produced wedges that occurred on the lateral and medial sides. The anterior-posterior impacts also produced wedges occurring on the lateral and medial sides. Kress (1989) stated that a vast majority of clinically seen femur impacts occur in the 1-m direction. With these additional findings, however, it is possible that a-p impacts may actually be mislabeled clinically as 1-m impacts.

Bending impact tests have been conducted on the intact thigh and will be reported on in a different paper. Now that the bare femur response is somewhat understood, the role of soft tissue and the role of the pelvis can be explored.

Test Series II: Torsional Strength of Femur

Low strain rate torsional tests were performed to develop a relationship between ultimate torque and cortical thickness. This relationship permitted the calculation of "percentage of maximum torque" values that established torsional preloads.

The tests clearly showed that even a small torsional preload reduced the breaking strength of the femur significantly. It also showed that a small torsional load (as compared to the impact load) can still result in a spiral fracture of the femur.

Test Series III: Compressive Strength of Femur

True axial loading in compression should produce only compressive stresses. However, in these axial experiments on the femur, tensile stresses resulting from bending could actually be the fracture initiators.

From the process of mapping out the stress on the bone, predicting the fracture, and showing the actual fracture location, it is obvious that bone geometry is the critical parameter in determining fracture location. In 14 out of 15 tests, the cross-section under the greatest calculated stress was the fracture site. Predictions were easy to make and extremely accurate.

A majority of the fractures (80 percent) occurred at the neck of the femur. This number appears high when compared to clinical studies where 50 percent of automobile accident victims (Daffner et al., 1988) and 17 percent of motorcycle victims (Deaner et al., 1975) with broken femurs have neck fractures. But when you consider age of the bones studied (the average age was 64.9 years), 80 percent neck fractures is not surprising. Osteoporosis attacks the femur in a disproportionate manner. The neck of the femur tends to lose bone at a higher rate than the rest of the femur (Hofeldt, 1987). As evidence of this, the three youngest bones tested broke at the shaft.

Fung (1984) reported a compressive strength in bone that is approximately 1.5 times greater than its tensile strength. Viewing the figures of mapped out stresses on the femur, it can be seen that the compressive stress on the medial side of the femur is always approximately 1.5 times the tensile stress on the lateral side of the femur.

The impact breaking strength was 39 percent greater than the breaking strength at very slow rates of load application. This change is significant and is almost exactly the change predicted by McElhaney (1966). This indicates that high-speed impact tests are necessary for studying automobile-motorcycle collisions.

The average breaking load for the slowly loaded bone was 5274 Newtons and for the impacted bones was 6464 Newtons. Present automobile design regulations dictate that a force of 10,000 Newtons may not be exceeded when a knee impacts a dashboard at 6.6 meters per second (Krishnaswamy, 1991). Results from this research indicate that this level might be high. Only one femur had a breaking tolerance higher than 10,000

Newtons.

More tests need to be performed in this area. Since a preponderance of neck fractures occur when using femurs of the elderly, young bones need to be tested. This is not as important in the other tests (1-m, a-p, torsion), since the bone geometry can be factored out using simple stress calculations. In these axial tests, however, the neck of old bones fracture before the shaft fracture threshold can be measured.

Test Series IV: Fresh Tissue Testing

Findings from this research, based on results from a small sample size, indicate that there is a significant change between fresh and embalmed properties. The fresh human femurs were 43.9 percent stronger than the embalmed femurs and absorbed 79.8 percent more energy. The difference in breaking strength for the tibias was even greater.

This conclusion must be viewed carefully. Only 14 fresh bones were tested. Also, these fresh bones came from individuals younger than the average embalmed bone donor.

More fresh tissue testing needs to be performed, and anatomical measurements need to be taken on the fresh tissue tested. This will help determine the exact difference between fresh and embalmed tissue.

Figures and Tables

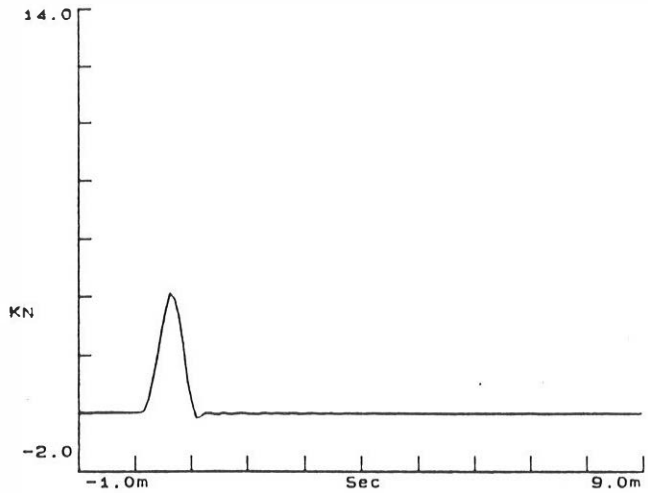

Figure 1 Sample force-time plot produced by crash simulator after impact.

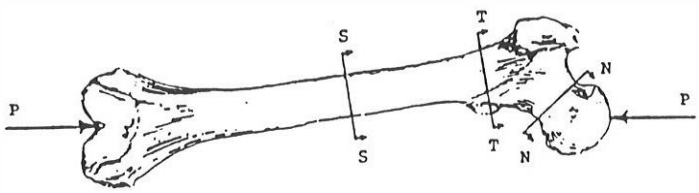

Figure 2 Diagram of axially loaded femur showing cross-sections of stress calculation: S = shaft, T = Trochanter, N = neck.

Table 1

Types of Fractures Occurring in
L-M Loaded Femurs

Fracture Type	Number	Percentage
Comminution		
Tension Wedge	5	41.7 %
Compression Wedge	1	8.3
Oblique	3	25.0
Spiral	2	16.7
Shatter	1	8.3

Table 2

Types of Fractures Occurring in
A-P Loaded Femurs

Fracture Type	Number	Percentage
Comminution		
Tension Wedge	3	9.6%
Compression Wedge	2	6.5
Side Wedge	17	54.8
Oblique	8	25.8
Shatter	1	3.2

Table 3

Independent Variables and Torque Data
on Femurs Loaded in Torsion at
Low Strain Rates

Bone	Cortex Thickness (meters)	Support Distance (meters)	Maximum Torque (N·m)
1	.00564	.381	96.0
2	.00758	.381	154.6
3	.00628	.318	113.8
4	.00894	.356	115.9
5	.00959	.387	145.0
6	.00201	.330	24.4
AVERAGE			108

Table 4

Independent Variables and Torque Data
for Femurs Loaded in L-M Bending
with Torsional Preload

Bone	Cortex Thickness (meters)	Support Distance (meters)	Torsional Preload (N·m)	Breaking Force (N)
RPFTU1L	.00611	.41	20.2	3657
RPFTU2L	.00586	.33	10.1	1355
RPFTU3L	.00702	.33	10.1	3335
RPFTNO2L	.00598	.33	10.1	1684
RPFTU4L	.00810	.34	20.2	1234
RPFTU5L	.00743	.36	20.2	1806

Table 5

Results from A-P Impact of Fresh Long
Bones of Two Individuals

Cadaver, bone	Breaking Force (N)
105	
Femur (right)	9482
Femur (left)	10017
Tibia (right)	6620
Tibia (left)	5542
Fibula (right)	930
Fibula (left)	772
Humerus (right)	5285
Humerus (left)	4469
98	
Femur (right)	7228
Femur (left)	6065
Tibia (right)	4988
Tibia (left)	4313
Fibula (right)	1129
Fibula (left)	895

Table 6

Summary of The Response Characteristics of The Human Femur

All bones were embalmed and impacted midshaft while simply-supported, unless noted otherwise

n	Impact Direction	Impactor	Average Force (kN)	Standard Deviation (kN)	Average Velocity (m/s)	Fracture Classifications		Remarks
2	A-P DW	4.13 cm Pipe	4.22	0.49	7.5	(n=2) 50.0% Tension Wedge	50.0% Comminuted	Impacted distal third
2	A-P	4.13 cm Pipe	1.00	0.64	Static	(n=2) 50.0% Tension Wedge	50.0% Transverse	Manual push
4	A-P	4.13 cm Pipe	8.20	1.86	6.6	(n=4) 50.0% Oblique	50.0% Transverse	Cryogenic Fresh. Thawed for test
30	A-P	4.13 cm Pipe	5.76	1.93	7.5	(n=32) 40.6% Comminuted 12.5% Segmental 6.3% Compression Wedge	15.6% Oblique 21.9% Side Wedge 3.1% Tension Wedge	
26*	*	*	5.78	1.41	7.5			* Specious values for #778L, 798R, 720L & 551L excluded in "n=26" #776L & 779L had no F recording
2	A-P	70 mm Snub	0.98	0.27	7.5	(n=2) Both Comminuted Longitudinal Segments		Drop-tower Impactor (DRI)
2	Pure Torsion	Pre-torque Device	58.1 N-m	53.7 N-m	Static	(n=2) Both Spiral Fractures.		Failed during pre-torque for "Pipe (Pre-T)" set-up
6	Pure Torsion	S-S Torsion	108.3 N-m	464 N-m	Static	(n=6) All S. trailfractures.		
5*	*	*	125.1 N-m	24.1 N-m	Static			* Specious value of #5 was excluded in "n=5"
4	L-M	4.13 cm Pipe (Pre-T)	2.86	1.70	7.0	(n=4) 75.0% Segmental	25.0% Oblique	Pre-torque of 20.34 N-m
3*	*	*	2.13	1.06	6.8			* Specious value of #695R was excluded in "n=3"
4	L-M	4.13 cm Pipe (Pre-T)	2.70	2.72	6.8	(n=6) 66.7% Spiral	33.3% Comminuted	Pre-torque of 10.06 N-m #668R and U7L had no recording of force
3*	*	*	1.57	1.84	6.8			* Specious value of #U6L was excluded in "n=3"
2	L-M PW	4.13 cm Pipe	5.60	1.63	7.5	(n=3) 33.3% Tension Wedge 33.4% Comminuted	33.3% Oblique	Impacted proximal third #997L had no recording of force
17	L-M	4.13 cm Pipe	3.16	1.89	7.1	(n=18) 27.8% Oblique 16.7% Tension Wedges 11.1% Compression Wedges	27.8% Segmental 11.1% Other Wedges 5.6% Comminuted	#679L had no recording of force
1	L-M	10cm Plate	4.57	na	7.5	(n=1) Compression Wedge		
10	Axial	10cm Plate	7.11	2.32	6.8	(n=10) 80.0% Involved Hip 40.0% Involved Shaft 20.0% Involved Knee		
8*	*	*	7.09	1.73	6.6			* Specious values for #557L and 4L were excluded in "n=8"
9	Axial	Materials Testing Machine	5.27	2.47	Static	(n=9) 88.9% Neck fractures. 11.1% Subtrochanteric fracture.		Compression testing of whole femur.
7*	*		5.01	1.44	Static			* Specious values for #859R and 812R were excluded in "n=7"

Table 7

Some Calculated Dynamic Response Characteristics from Selected Data of the Human Femur

All bones and intact specimens were embalmed and impacted while simply-supported, unless noted otherwise.

FEMUR (Avg. Cortex Thickness = 5.75 mm)						
12	L-M	4.13 cm Pipe	3.05	7.6	41.7% comminuted (tension wedge most prevalent)	Bending Strength = 147 MPa Young's Modulus = 30 GPa Energy = 2,236 N-ms
30	A-P	4.13 cm Pipe	5.70	7.5	70.9% comminuted (side wedge most prevalent)	Bending Strength = 284 MPa Young's Modulus = 88 GPa Energy = 2,658 N-ms
5	Pure Torsion	S-S Torsion	125.1 N-m	Static	All spiral fractures	Torsional Stress = 26 MPa
9	Axial	Materials Testing Machine	5.27	Static	88.9% Neck fractures 11.1% Subtrochantric fractures	Compressive Stress = 125 MPa Tensile Stress = 79 MPa Compressive Strength is 1.5 times >tensile strength
6	Axial	10 cm Plate	6.46	7.6	80.0% Involved Hip 40.0% Involved Shaft 20.0% Involved Knee	Compressive Stress = 174 MPa Tensile Stress = 121 MPa

Bibliography

Chapman, Michael W. "Concomitant Ipsilater Fractures of the Hip and Femur." The Multiply Injured Patient with Complex Fractures, Meyers, Marvin H., Editor, Philadelphia: Lea and Febiger, 1984.

Daffner, Richard H., et al. "Patterns of High-Speed Impact Injuries in Motor Vehicle Occupants." Journal of Trauma, 28(1988), pp. 498-501.

Deaner, R.M., and V.H. Fitchett. "Motorcycle Trauma." Journal of Trauma, 15(1975), pp. 678-681.

Evans, F.G., and M. Lebow. "Regional Differences in Some of the Physical Properties of Human Femur." J. Applied Physiol., 2(1951), pp. 563-572.

Fung, Y.C. Biomechanics - Mechanical Properties of Living Tissues. New York: Springer-Verlag, 1981.

Hofeldt, Fred. "Proximal Femoral Fractures." Clinical Orthopaedics and Related Research, 1987, pp. 12-18.

Kress, Tyler A. "Mechanical Behavior of Lower Limbs in Reponse to Impact Loading: Facility Development and Initial Results." Master of Science Thesis in Engineering Science, The University of Tennessee, Knoxville, 1989.

Krishnaswamy, Prakash, et al. "Crash Codes Pave the Way to Safer Vehicles." Mechanical Engineering, 113(1991), pp. 60-62.

Mather, B. S. "Variation with Age and Sex in Strength of the Femur." Med. and Biol. Engr., 6(1968), pp. 129-132.

McElhaney, James H. "Dynamic Response of Bone and Muscle Tissue." Journal of Applied Physiology, 21(1966), pp. 1231-1236.

Moore, Keith L. Clinically Oriented Anatomy. Baltimore: Williams and Wilkins, 1985.

Tucker, Guy V. "The Mechanical Behavior of the Human Femur Subjected to Impact Loading." Master of Science Thesis in Engineering Science, The University of Tennessee, Knoxville, 1991.

Viano, D.C., and T.B. Khalil. "Investigation of Impact Response and Fracture of the Human Femur by finite Element Modeling." Proceedings Mathematical Modeling Biodynamic Response to Impact. Society of Automotive Engineers, Inc., 760773, 1976, pp. 53-60.

Acknowledgment

The Japan Automobile Manufacturers Association (JAMA) is the sole sponsor of the research project entitled, "Dynamic Response of the Human Leg to Impact Loading."